Measurement of event-by-event flow harmonics in Pb-Pb Collisions at $\sqrt{s_{\mathrm{NN}}}$=2.76 TeV with the ATLAS detector

Jiangyong Jia (on behalf of the ATLAS Collaboration)[1]

Chemistry Department, Stony Brook University, NY 11794, USA; Physics Department, Brookhaven National Laboratory, NY 11796, USA

Abstract

The event-by-event distributions of harmonic flow coefficients v_n for n=2–4 are measured in Pb-Pb collisions at $\sqrt{s_{NN}}$ = 2.76 TeV, using charged particles with $p_{\mathrm{T}} > 0.5$ GeV and $|\eta| < 2.5$. The shape of the v_n distributions is consistent with Gaussian fluctuations in central collisions for v_2 and over the measured centrality range for v_3 and v_4. When these distributions are rescaled to the same $\langle v_n \rangle$, the resulting shapes are similar for $p_{\mathrm{T}} > 1$ GeV and $0.5 < p_{\mathrm{T}} < 1$ GeV. The shape of the eccentricity distributions from Glauber and the MC-KLN models fail to describe the shape of the v_n distributions over the full centrality range.

In recent years, the measurement of harmonic flow coefficients v_n has provided important insight into the hot and dense matter created in heavy ion collisions at RHIC and the LHC. These coefficients are generally obtained from a Fourier expansion of particle azimuthal angle distributions, $\frac{dN}{d\phi} \propto 1+2\sum_{n=1}^{\infty} v_n \cos n(\phi-\Phi_n)$, where Φ_n represents the phase of v_n (event plane or EP) [1, 2]. Previous measurements determined the v_n from the distribution of $\phi-\Phi_n$, accumulated over many events. This event-averaged v_n mainly reflects the hydrodynamic response of the created matter to the average collision geometry in the initial state. However, more information can be obtained by measuring the v_n on a event-by-event (EbE) basis, such as the nature of the EbE fluctuations in the initial geometry. This proceedings present the methods and results of EbE v_n for $n = 2-4$ obtained with the ATLAS detector [3].

This analysis is based on 8 μb^{-1} of minimum bias Pb-Pb data collected in 2010 at $\sqrt{s_{\mathrm{NN}}}$ = 2.76 TeV [4]. The v_n coefficients are calculated using tracks with $p_{\mathrm{T}} > 0.5$ GeV and $|\eta| < 2.5$, reconstructed by the inner detector (ID). To illustrate the level of EbE fluctuations, Figure 1 shows the distributions of track ϕ and track pair relative angle $\Delta\phi$ with $p_{\mathrm{T}} > 0.5$ GeV for three central events. Rich EbE patterns, beyond the structures of the detector acceptance (solid points) and statistical fluctutions, are observed. These distributions are the inputs for the EbE v_n analyses.

Two methods are used to obtain the EbE v_n. The first method starts with a Fourier expansion of the azimuthal distribution of charged particles in a given event, reweighted by the inverse of the tracking efficiency for each particle:

$$\frac{dN}{d\phi} \propto 1 + 2\sum_{n=1}^{\infty} v_n^{\mathrm{obs}} \cos n(\phi - \Phi_n^{\mathrm{obs}}) = 1 + 2\sum_{n=1}^{\infty}\left(v_{n,\mathrm{x}}^{\mathrm{obs}} \cos n\phi + v_{n,\mathrm{y}}^{\mathrm{obs}} \sin n\phi\right), v_n^{\mathrm{obs}} = \sqrt{\left(v_{n,\mathrm{x}}^{\mathrm{obs}}\right)^2 + \left(v_{n,\mathrm{y}}^{\mathrm{obs}}\right)^2}, \quad (1)$$

where v_n^{obs} is the magnitude of the observed per-particle flow vector: $\vec{v}_n^{\,\mathrm{obs}} = (v_{n,\mathrm{x}}^{\mathrm{obs}}, v_{n,\mathrm{y}}^{\mathrm{obs}})$. In the limit of infinite multiplicity and the absence of non-flow effects, it approaches the true flow

[1] A list of members of the ATLAS Collaboration and acknowledgements can be found at the end of this issue.

Preprint submitted to Nuclear Physics A *October 23, 2012*

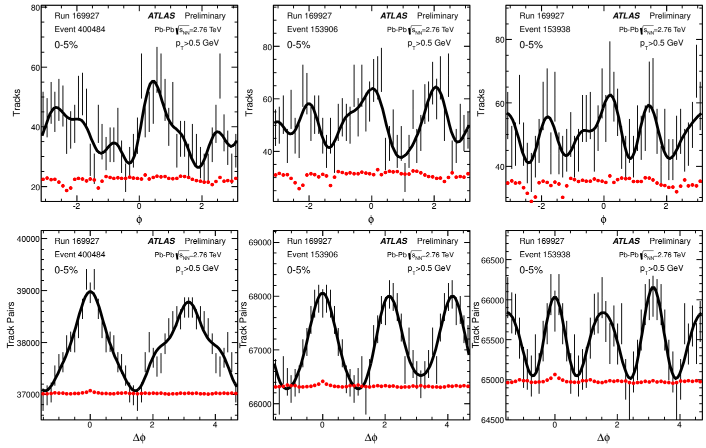

Figure 1: Single track ϕ (top) and track pair $\Delta\phi$ (bottom) distributions for three events (from left to right) in 0-5% centrality interval [4]. The pair distributions have been folded into [-0.5π,1.5π]. The bars indicate the statistical uncertainties, the solid curves indicate a Fourier parameterization including first six harmonics: $dN/d\phi = A(1 + 2\sum_{i=1}^{6} c_n \cos n(\phi - \Psi_n))$ for single track distributions and $dN/d\Delta\phi = A(1 + 2\sum_{i=1}^{6} c_n \cos n(\Delta\phi))$ for pair distributions, and the red solid points indicate the acceptance functions (arbitrary normalization).

signal: $v_n^{\mathrm{obs}} \to v_n$. The key of the measurement is to determine the response function $p(\vec{v}_n^{\mathrm{obs}}|\vec{v}_n)$ or $p(v_n^{\mathrm{obs}}|v_n)$, used to unfold these smearing effects.

In order to determine the response function, the tracks in the ID are divided into two subevents with symmetric η range, $\eta > 0$ and $\eta < 0$. The smearing effects are estimated from the difference of the flow vectors between the two subevents, for which the physical flow signal cancels, but with a smearing that is $\sqrt{2}$ larger. This distribution is observed to be well described by a 2-D Gaussian with equal widths in both dimensions, thus a simple shift to $\vec{v}_n = (v_{n,\mathrm{x}}, v_{n,\mathrm{y}})$, followed by an integration over the azimuthal angle, gives the desired 1-D response function [5]:

$$p(v_n^{\mathrm{obs}}|v_n) \propto v_n^{\mathrm{obs}} e^{-\frac{(v_n^{\mathrm{obs}})^2 + v_n^2}{2\delta^2}} I_0\left(\frac{v_n^{\mathrm{obs}} v_n}{\delta^2}\right), \delta = \begin{cases} \delta_{\mathrm{2SE}}/\sqrt{2} & \text{for half-ID} \\ \delta_{\mathrm{2SE}}/2 & \text{for full-ID} \end{cases} \tag{2}$$

where I_0 is the modified Bessel function of the first kind and $s = v_n^{\mathrm{obs}} - v_n$ denotes the smearing.

In the second method, the observed flow signal is defined from an EbE pair distribution, obtained by convolving the tracks in the first half-ID with those in the second half-ID:

$$\frac{dN}{d\Delta\phi} \propto \left[1 + 2\sum_n \left(v_{n,\mathrm{x}}^{\mathrm{obs_1}} \cos n\phi_1 + v_{n,\mathrm{y}}^{\mathrm{obs_1}} \sin n\phi_1\right)\right] \otimes \left[1 + 2\sum_n \left(v_{n,\mathrm{x}}^{\mathrm{obs_2}} \cos n\phi_2 + v_{n,\mathrm{y}}^{\mathrm{obs_2}} \sin n\phi_2\right)\right] \tag{3}$$

$$= 1 + 2\sum_n (A_n \cos n\Delta\phi + B_n \sin n\Delta\phi)\,, \quad v_n^{\mathrm{obs,2PC}} = \left(A_n^2 + B_n^2\right)^{1/4} = \sqrt{v_n^{\mathrm{obs_1}} v_n^{\mathrm{obs_2}}} = \sqrt{(v_n + s_1)(v_n + s_2)}$$

where $s_1 = v_n^{\mathrm{obs_1}} - v_n$ and $s_2 = v_n^{\mathrm{obs_2}} - v_n$ are independent variables described by the probability distribution in Eq. 2 with $\delta = \delta_{\mathrm{2SE}}/\sqrt{2}$. The response function for $v_n^{\mathrm{obs,2PC}}$ is different from v_n^{obs} due to the presence of two random variables.

The Bayesian unfolding procedure from [6] is used to calculate the v_n distribution, in three p_{T} ranges: $p_{\mathrm{T}} > 0.5$ GeV, $1 > p_{\mathrm{T}} > 0.5$ GeV and $p_{\mathrm{T}} > 1$ GeV. In each case, the prior (initial distribution) is taken as the v_n^{obs} distribution from the full-ID, and the number of iterations N_{iter} is chosen according to the sample statistics and binning. The convergence is generally reached for $N_{\mathrm{iter}} \geq 8$ in the case of $n = 2$, but more iterations are required for $n > 2$ and in more peripheral collisions. The results are also found to be independent of the choice of priors, the size of the detector, as well as the two unfolding methods used.

Figure 2 shows the probability distribution of the EbE v_n in several centrality intervals obtained for charged particles at $p_{\mathrm{T}} > 0.5$ GeV. The shape of these distributions changes strongly with centrality for v_2, while it is relatively unchanged for higher-order harmonics. These distributions are compared with the PDF obtained by radial projection of a 2-D Gaussian distribution in $\vec{v}_n$: $P(v_n) = \frac{v_n}{\sigma^2} e^{-\frac{v_n^2}{2\sigma^2}}, \sigma = \sqrt{\frac{2}{\pi}}\langle v_n \rangle$. The Gaussian description works well for v_3 and v_4 over the measured centrality range, but fails for v_2 beyond the top 2% most central collisions.

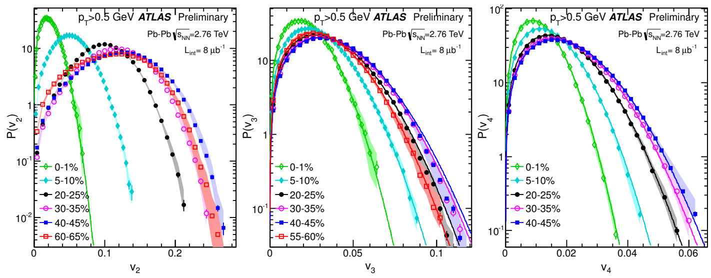

Figure 2: The probability distribution of the EbE v_n for $n = 2$ (left), $n = 3$ (middle) and $n = 4$ (right) [4]. The solid curves are Gaussian distributions with mean adjusted to the measured $\langle v_n \rangle$, shown for the 0-1% centrality interval for v_2, but for all centrality intervals for v_3 and v_4.

Many quantities can be calculated directly from these distributions, such as the mean $\langle v_n \rangle$, width σ_{v_n}, ratio $\sigma_{v_n}/\langle v_n \rangle$ and RMS value $\sqrt{\langle v_n^2 \rangle} \equiv \sqrt{\langle v_n \rangle^2 + \sigma_{v_n}^2}$. The $\sigma_{v_n}/\langle v_n \rangle$ is a measure of the relative fluctuations of v_n and was previously estimated from two- and four-particle cumulant methods [7]. Figure 3 shows that the $\sigma_{v_n}/\langle v_n \rangle$ calculated for the three p_T ranges are remarkably stable, suggesting that the hydrodynamic response to the initial geometry is nearly independent of p_T. For v_2, the values of $\sigma_{v_n}/\langle v_n \rangle$ vary strongly with $\langle N_{part} \rangle$, and reach a minimum of about 0.34 at $\langle N_{part} \rangle \sim 200$ or 20-30% centrality range. For v_3 and v_4, the values of $\sigma_{v_n}/\langle v_n \rangle$ are almost independent of $\langle N_{part} \rangle$, and are consistent with the value expected from Gaussian distributions.

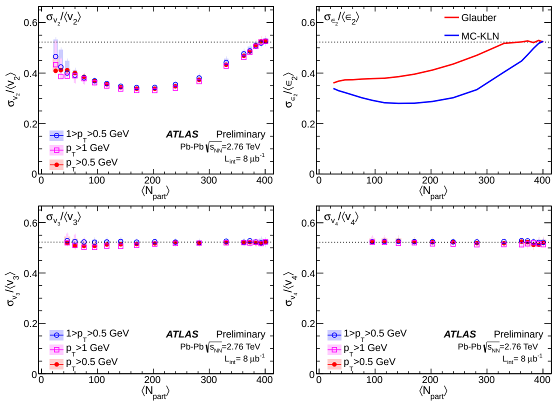

Figure 3: The $\sigma_{v_n}/\langle v_n \rangle$ vs. $\langle N_{part} \rangle$ in three p_T ranges for $n = 2$ (top-left), $n = 3$ (bottom-left) and $n = 4$ (bottom-right) [4]. The dotted lines indicate $\sqrt{4/\pi - 1} \approx 0.523$ expected for Gaussian fluctuations. Top-right panel shows the $\sigma_{\epsilon_2}/\langle \epsilon_2 \rangle$ for the Glauber model [8] and the MC-KLN model [9].

Figure 4 compares the EbE v_2 distributions with the distributions of the eccentricity ϵ_2 of the initial geometry, calculated for the Glauber model [8] and the MC-KLN model (version 3.46) [9]. The ϵ_2 distribution for each centrality interval is rescaled to match the $\langle v_2 \rangle$ of the data, and then normalized into a PDF. Figure 4 shows that the rescaled ϵ_2 distributions describe the data well for the most central collisions, but start to fail in non-central collisions. This behavior is also reflected in the comparison of $\sigma_{v_2}/\langle v_2 \rangle$ with $\sigma_{\epsilon_2}/\langle \epsilon_2 \rangle$ in the top-right panel of Figure 3. The agreement with the models for $n = 3 - 4$ (see [4] for more details) are better than the $n = 2$ case, however, this could simply reflect the fact that all distributions are dominated by Gaussian fluctuations, which have a universal shape.

The EP method in general is known to measure a v_n value between the simple average and the RMS of the true v_n [10]: $\langle v_n \rangle \leq v_n^{EP} \leq \sqrt{\langle v_n^2 \rangle}$. This relation is checked explicitly in Figure 5 based on the EbE v_n distributions. For v_3 and v_4, the values of v_n^{EP} are almost identical to $\sqrt{\langle v_n^2 \rangle}$; For v_2, the values of v_2^{EP} are in between $\langle v_n \rangle$ and $\sqrt{\langle v_n^2 \rangle}$: they are closer to $\langle v_n \rangle$ in mid-central collisions

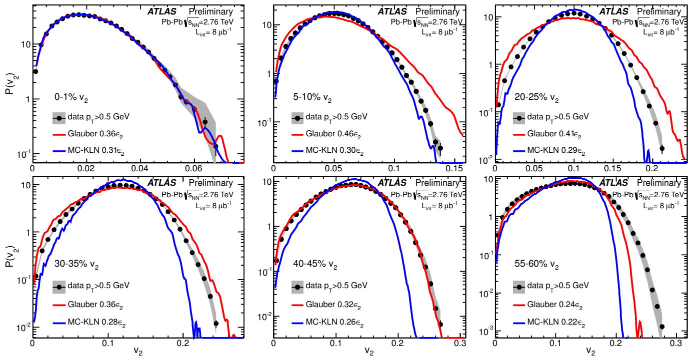

Figure 4: The EbE v_2 distributions compared with the ϵ_2 distributions from the Glauber model (red lines) and the MC-KLN model (blue lines) [4].

where the EP resolution factor is close to one, and approach $\sqrt{\langle v_n^2 \rangle}$ in peripheral collisions where the resolution factor is small.

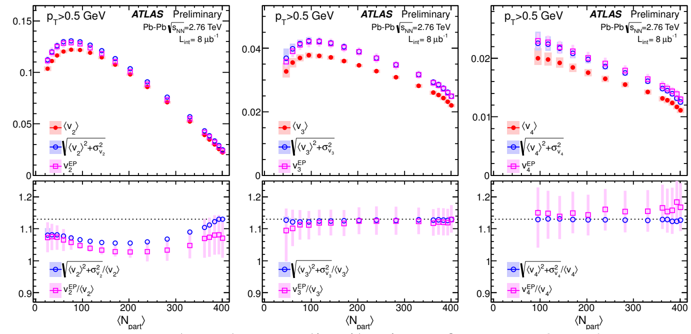

Figure 5: Top panels: Comparison of $\langle v_n \rangle$ and $\sqrt{\langle v_n^2 \rangle} \equiv \sqrt{\langle v_n \rangle^2 + \sigma_{v_n}^2}$ with v_n^{EP} [4]. Bottom panels: the ratios of $\sqrt{\langle v_n^2 \rangle}$ and v_n^{EP} to $\langle v_n \rangle$ [4]. The dotted lines in bottom panels at $\sqrt{\langle v_n^2 \rangle}/\langle v_n \rangle = \sqrt{4/\pi} \approx 1.13$ indicate the value expected for Gaussian fluctuations.

In summary, the EbE v_n distributions for $n = 2 - 4$ are measured for Pb-Pb collision at $\sqrt{s_{\mathrm{NN}}} = 2.76$ TeV. The shape of the v_n distributions is consistent with Gaussian fluctuation in central collisions (0-2% centrality range) for v_2 and over the full centrality range for v_3 and v_4. The ratio of the RMS to the mean, $\sigma_{v_n}/\langle v_n \rangle$, is studied as a function of $\langle N_{\mathrm{part}} \rangle$ and p_{T}. The values of $\sigma_{v_n}/\langle v_n \rangle$ are found to be independent of p_{T}, suggesting that the hydrodynamic response to the eccentricity of the initial geometry has little p_{T} dependence, however they are found to reach a minimum of 0.34 for v_2 around $\langle N_{\mathrm{part}} \rangle \sim 200$. A comparison of the v_n distributions with the eccentricity distributions of the initial geometry from the Glauber and MC-KLN models, shows that both models fail to describe the data across the full centrality range. The v_n from the event plane method is found to lie in between $\langle v_n \rangle$ and $\sqrt{\langle v_n \rangle^2 + \sigma_{v_n}^2}$. These results may shed light on the nature of the fluctuations of the created matter in the initial state as well as the subsequent hydrodynamic evolution.

This work is in part supported by NSF under award number PHY-1019387.

References

[1] ATLAS Collaboration, Phys. Rev. C **86**, 014907 (2012), arXiv:1203.3087 [hep-ex].
[2] ATLAS Collaboration, https://cdsweb.cern.ch/record/1451882, arXiv:1208.1427 [nucl-ex].
[3] ATLAS Collaboration, JINST **3**, S08003 (2008).
[4] ATLAS Collaboration, ATLAS-CONF-2012-114, https://cdsweb.cern.ch/record/1472935.
[5] J. -Y. Ollitrault, Phys. Rev. D **46**, 229 (1992).
[6] G. D'Agostini, Nucl. Instrum. Meth. A **362**, 487 (1995); T. Adye, arXiv:1105.1160 [physics.data-an].
[7] ALICE Collaboration, J. Phys. G G **38**, 124013 (2011), arXiv:1106.6284 [nucl-ex].
[8] M. L. Miller, *et.al.* Ann. Rev. Nucl. Part. Sci. **57**, 205 (2007), arXiv:nucl-ex/0701025.
[9] H. J. Drescher and Y. Nara, Phys. Rev. C **75**, 034905 (2007); MC-KLN 3.46 at http://www.aiu.ac.jp/~ynara/mckln/.
[10] PHOBOS Collaboration, Phys. Rev. C **77**, 014906 (2008).